ACS OMEGA

http://pubs.acs.org/journal/acsodf

Article

Preclinical Pharmacokinetics of Complement C5a Receptor Antagonists PMX53 and PMX205 in Mice

Vinod Kumar, John D. Lee, Richard J. Clark, Peter G. Noakes, Stephen M. Taylor, and Trent M. Woodruff*

Cite This: *ACS Omega* 2020, 5, 2345−2354

Read Online

ACCESS | Metrics & More | Article Recommendations

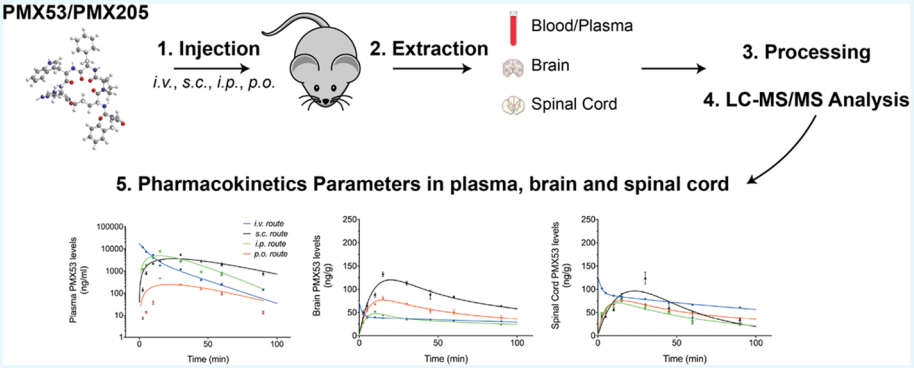

ABSTRACT: The cyclic hexapeptides PMX53 and PMX205 are potent noncompetitive inhibitors of complement C5a receptor 1 (C5aR1). They are widely utilized to study the role of C5aR1 in mouse models, including central nervous system (CNS) disease, and are dosed through a variety of routes of administration. However, a comprehensive pharmacokinetics analysis of these drugs has not been reported. In this study, the blood and CNS pharmacokinetics of PMX53 and PMX205 were performed in mice following intravenous, intraperitoneal, subcutaneous, and oral administration at identical doses. The absorption and distribution of both drugs were rapid and followed a two-compartment model with elimination half-lives of ∼20 min for both compounds. Urinary excretion was the major route of elimination following intravenous dosing with ∼50% of the drug excreted unchanged within the first 12 h. Oral bioavailability of PMX205 was higher than that of PMX53 (23% versus 9%), and PMX205 was also more efficient than PMX53 at entering the intact CNS. In comparison to other routes, subcutaneous administration of PMX205 resulted in high bioavailability (above 90%), as well as prolonged plasma and CNS exposure. Finally, repeated daily oral or subcutaneous administration of PMX205 demonstrated no accumulation of drug in blood, the brain, or the spinal cord, promoting its safety for chronic dosing. These results will be helpful in correlating the desired therapeutic effects of these C5aR1 antagonists with their pharmacokinetic profile. It also suggests that subcutaneous dosing of PMX205 may be an appropriate route of administration for future clinical testing in neurological disease.

1. INTRODUCTION

The complement system is a vital component of the immune system that "complements" antibodies and phagocytic cells in their ability to clear pathogens and respond to sterile injury. Once stimulated by one of several triggers, it leads to a cascade of various enzymatic sequences that generate opsonin, intermediate complement "anaphylatoxin" peptides, and the terminal membrane attack complex.[1] The most potent inflammatory complement fragment, C5a, exhibits various immunoregulatory and pro-inflammatory biological activities[2] by binding to two known receptors, termed C5a receptor 1 (C5aR or CD88, now referred to as *C5aR1*) and C5a receptor-like 2 (C5L2 or GPR77, now referred to as *C5aR2*).[3] On most cells, expression levels of C5aR1 are higher than C5aR2, and its activation drives disease pathology, including diseases affecting the CNS.[2,4−7] The discovery and development of selective C5aR1 inhibitors have therefore been an active area of research for many decades.

Although there are several C5aR1-targeted therapeutics in development for various diseases,[8] few have achieved widespread use amongst researchers as compared to the class of

Received: November 4, 2019
Accepted: January 21, 2020
Published: January 30, 2020

https://dx.doi.org/10.1021/acsomega.9b03735
ACS Omega 2020, 5, 2345−2354

Table 1. Plasma Pharmacokinetic Parameters of Complement C5a Receptor 1 Antagonists[a]

		PMX53				PMX205			
parameters	units	i.v.	s.c.	i.p.	p.o.	i.v.	s.c.	i.p.	p.o.
Cmax	μg/mL	17.42	3.77	4.92	0.25	34.62	5.62	5.95	0.77
Tmax	min		27.22	14.28	21.91		27.98	14.28	27.72
Vss	mL	2.90				2.76			
V1_F	mL	1.72	<0.01	<0.01	0.05	0.87	<0.01	<0.01	0.01
CL_F	μL/min	199.16	0.11	0.16	2.01	146.90	0.07	0.13	0.52
V2_F	mL	1.05	<0.01	<0.01	<0.01	2.04	<0.01	<0.01	<0.01
CLD2_F	μL/min	84.57	<0.01	<0.01	<0.01	197.45	<0.01	<0.01	<0.01
K01	1/h		2.28	4.29	2.92		2.21	4.30	2.24
K10	1/h	6.94	2.13	4.11	2.56	10.17	2.08	4.10	2.09
K12	1/h	2.95	<0.001	<0.001	<0.001	13.67	<0.001	<0.001	<0.001
K21	1/h	4.85	2.14	2.00	2.58	5.82	2.08	2.00	2.09
K01_HL	min		18.28	9.70	14.23		18.85	9.67	18.55
K10_HL	min	5.99	19.47	10.10	16.22	4.09	19.93	10.13	19.85
Alpha	1/min	0.20	0.04	0.07	0.04	0.46	0.03	0.07	0.03
Beta	1/min	0.05	0.04	0.03	0.04	0.04	0.03	0.03	0.03
Alpha_HL	min	3.49	19.53	10.11	16.32	1.51	20.00	10.14	19.92
Beta_HL	min	14.73	19.42	20.75	16.02	19.33	19.92	20.75	19.87
MRT_last	min	13.21	38.77	27.43	32.61	19.74	40.71	24.78	37.68
MRT_INF_obs	min	18.03	47.94	36.15	33.97	37.00	64.30	26.30	54.41
MRT_INF_pred	min	17.92	48.13	36.08	34.07	37.29	64.29	26.34	54.19

[a]Cmax: peak plasma drug concentration; Tmax: time to reach peak plasma concentration following drug administration; Vss: apparent volume of distribution at a steady state; V1_F and V2_F: apparent volume of central and peripheral compartments in two compartmental models; CL_F and CLD2_F: apparent total body clearance of the drug from plasma and apparent total clearance of the drug from plasma after administration; K01: absorption rate constant; K10: elimination rate constant; K12 and K21: distribution and redistribution rate constant; K01_HL and K10_HL: distribution half-life and elimination half-life; Alpha and Beta: hybrid first-order rate constants expressing initial and terminal slopes of distribution and elimination phases; Alpha_HL and Beta_HL: initial or disposition half-life and terminal elimination half-life; MRT_last, MRT_INF_obs, and MRT_INF-pred: mean residence time at the last time point, infinity observed, and infinity predicted using two-compartmental analysis.

Table 2. Brain Pharmacokinetic Parameters of Complement C5a Receptor 1 Antagonists[a]

		PMX53				PMX205			
parameters	units	i.v.	s.c.	i.p.	p.o.	i.v.	s.c.	i.p.	p.o.
Cmax	ng/g	74.13	120.37	48.08	76.99	76.99	161.76	155.70	153.70
Tmax	min		19.87	10.45	14.89		30.23	19.85	20.71
Vss	μg/(ng/g)	0.74				0.54			
V1_F	μg/(ng/g)	0.40	0.15	0.31	0.31	0.13	0.08	0.08	0.18
CL_F	ng/(min ng/g)	2.43	1.75	3.77	2.28	2.56	1.66	1.27	0.75
V2_F	μg/(ng/g)	0.33	0.08	0.40	0.16	0.41	0.07	0.19	<0.001
CLD2_F	ng/(min ng/g)	107.59	2.91	25.61	2.68	43.73	0.70	2.71	<0.001
K01	1/h		5.81	9.06	11.20		2.35	3.81	11.27
K10	1/h	0.36	0.68	0.72	0.44	1.16	1.26	0.90	0.25
K12	1/h	15.95	1.13	4.92	0.51	19.79	0.53	1.92	<0.001
K21	1/h	19.41	2.07	3.87	0.99	6.40	0.61	0.87	2.88
K01_HL	min		7.16	4.59	3.71		17.71	10.91	3.69
K10_HL	min	115.54	60.95	57.39	94.86	35.89	32.91	46.56	165.07
Alpha	1/h	35.52	3.48	9.22	1.68	27.08	2.03	3.45	2.88
Beta	1/h	0.20	0.41	0.30	0.26	0.27	0.38	0.23	0.25
Alpha_HL	h	0.02	0.20	0.08	0.41	0.03	0.34	0.20	0.24
Beta_HL	h	3.52	1.71	2.28	2.69	2.53	1.83	3.08	2.75
MRT_last	h	0.70	0.70	0.68	0.68	0.64	0.72	0.66	0.75
MRT_INF_obs	h	5.46	1.98	2.29	1.89	3.88	1.85	1.24	2.43
MRT_INF_pred	h	5.45	1.97	2.30	1.88	3.88	1.82	1.24	2.44

[a]Cmax: peak drug concentration; Tmax: time to reach peak concentration following drug administration; Vss: apparent volume of distribution at a steady state; V1_F and V2_F: apparent volume of central and peripheral compartments in two compartmental models; CL_F and CLD2_F: apparent total body clearance of the drug and apparent total clearance of the drug after administration; K01: absorption rate constant; K10: elimination rate constant; K12 and K21: distribution and redistribution rate constant; K01_HL and K10_HL: distribution half-life and elimination half-life; Alpha and Beta: hybrid first-order rate constants expressing initial and terminal slopes of distribution and elimination phases; Alpha_HL and Beta_HL: initial or disposition half-life and terminal elimination half-life; MRT_last, MRT_INF_obs, and MRT_INF-pred: mean residence time at the last time point, infinity observed, and infinity predicted using two-compartmental analysis.

https://dx.doi.org/10.1021/acsomega.9b03735
ACS Omega 2020, 5, 2345−2354

Table 3. Spinal Cord Pharmacokinetic Parameters of Complement C5a Receptor 1 Antagonists[a]

		PMX53				PMX205			
parameters	units	i.v.	s.c.	i.p.	p.o.	i.v.	s.c.	i.p.	p.o.
Cmax	ng/g	129.82	96.56	71.26	75.88	449.84	225.14	219.65	214.33
Tmax	min		23.15	11.86	14.89		45.90	17.48	63.47
Vss	μg/(ng/g)	0.33				0.27			
V1_F	μg/(ng/g)	0.23	0.12	0.35	0.32	0.07	0.05	0.06	0.05
CL_F	ng/(min ng/g)	1.52	3.68	5.15	2.33	1.63	1.00	0.99	0.81
V2_F	μg/(ng/g)	0.10	0.26	<0.01	0.16	0.20	0.05	0.14	<0.001
CLD2_F	ng/(min ng/g)	30.58	1.36	0.01	2.71	21.89	0.07	2.59	<0.001
K01	1/hr		2.70	15.39	11.20		1.34	4.45	0.99
K10	1/hr	0.40	1.87	0.87	0.44	1.46	1.25	1.05	0.90
K12	1/hr	7.94	0.69	<0.01	0.51	19.69	0.08	2.75	<0.01
K21	1/hr	18.30	0.32	0.19	1.00	6.59	0.32	1.08	0.33
K01_HL	min		15.39	2.70	3.71		30.93	9.36	42.04
K10_HL	min	105.04	22.22	47.70	94.33	28.39	34.79	39.53	46.04
Alpha	1/hr	26.36	2.66	0.87	1.69	27.40	1.28	4.64	0.90
Beta	1/hr	0.27	0.22	0.19	0.26	0.35	0.32	0.24	0.33
Alpha_HL	hr	0.03	0.26	0.79	0.41	0.03	0.55	0.15	0.77
Beta_HL	hr	2.52	3.09	3.71	2.66	1.97	2.16	2.84	2.08
MRT_last	hr	0.69	0.64	0.62	0.68	0.62	0.81	0.65	0.80
MRT_INF_obs	hr	4.86	1.49	1.16	1.89	2.45	2.71	1.34	1.06
MRT_INF_pred	hr	4.86	1.46	1.13	1.88	2.45	2.69	1.31	1.07

[a]Cmax: peak drug concentration; Tmax: time to reach peak concentration following drug administration; Vss: apparent volume of distribution at a steady state; V1_F and V2_F: apparent volume of central and peripheral compartment in two compartmental models; CL_F and CLD2_F: apparent total body clearance of the drug and apparent total clearance of the drug after administration; K01: absorption rate constant; K10: elimination rate constant; K12 and K21: distribution and redistribution rate constant; K01_HL and K10_HL: distribution half-life and elimination half-life; Alpha and Beta: hybrid first-order rate constants expressing initial and terminal slopes of distribution and elimination phases; Alpha_HL and Beta_HL: initial or disposition half-life and terminal elimination half-life; MRT_last, MRT_INF_obs, and MRT_INF-pred: mean residence time at the last time point, infinity observed, and infinity predicted using two-compartmental analysis.

cyclic peptide C5aR1 inhibitors discovered at The University of Queensland over 20 years ago. These well-studied inhibitors, Ac-Phe-[Orn-Pro-dCha-Trp-Arg] (3D53 or PMX53)[9] and hydrocinnamate-[Orn-Pro-dCha-Trp-Arg] (PMX205),[10] are cyclic peptide compounds that act in a pseudo-irreversible and insurmountable manner at nanomolar concentrations targeting complement C5aR1. PMX205 is a lipophilic analogue of PMX53, with a substitution of a hydrocinnamate residue for the extracylic phenylalanine residue. It is known to exhibit enhanced efficacy and in vivo stability compared to its parent molecule PMX53.[7,10−13] As such, PMX205 has been suggested as a more ideal drug candidate for human disease, including neurological disorders. Indeed this drug has shown beneficial effects in rodent models of striatal neurodegeneration,[7] amyotrophic lateral sclerosis,[4,11] spinal cord injury,[5,14] and reduction of memory loss in mice with Alzheimer's disease.[15,16] For more than 15 years, both antagonists have been used by multiple laboratories in numerous experimental inflammatory conditions. Despite being peptidic molecules, their cyclic nature enables them to demonstrate a number of favorable properties required for clinical development such as high receptor selectivity, nanomolar potency, stability, oral bioavailability, and ability to cross neuroprotective barriers.[7,17,18] Additionally, oral and topical PMX53 has also successfully completed early phase I human clinical trials, demonstrating the potential human safety of this class of compounds.[19]

Despite the widespread usage of these C5aR1 antagonists, only a few studies have reported the quantitative pharmacokinetic determination of these antagonists.[6,12,20−22] A drawback to these prior pharmacokinetic studies is that the time points collected were minimal and not sufficient to observe a full pharmacokinetic profile to obtain accurate half-lives and elimination values and various other pharmacokinetic parameters. Furthermore, no prior study has performed tissue distribution studies or correlated drug pharmacokinetics via different routes of administration. Therefore, the purpose of the present study was to perform a complete pharmacokinetic analysis of these antagonists in healthy mice via various routes of drug administration, at the same dose, using a validated bioanalytical quantitative LC−MS/MS method.[13]

2. RESULTS

2.1. Pharmacokinetics of C5aR1 Antagonists in Wild-Type Mice. PMX53 and PMX205 levels obtained from LC−MS/MS analysis were corrected for process efficiency, extraction efficiency, and recovery correction factors as described previously.[13] Plasma concentration versus time profile data obtained from raw data for both antagonists demonstrated a curvilinear profile on a semi-log scale, a reflection that both antagonists undergo fast distribution and elimination phases and are best fitted to a two-compartment open model. The two-compartment pharmacokinetic model of WINNONLIN was therefore utilized for calculation of the various pharmacokinetic parameters for plasma, the brain, and the spinal cord with the resulting data presented in Tables 1−3.

Fitness of the pharmacokinetic model was assessed using in-built diagnostics of WINNONLIN software, Akaike Information Criterion, and by plotting the predicted curve as a function of time, with the observed concentrations overlaid on the plot indicating close correlation of the values (Figure 1).

https://dx.doi.org/10.1021/acsomega.9b03735
ACS Omega 2020, 5, 2345−2354

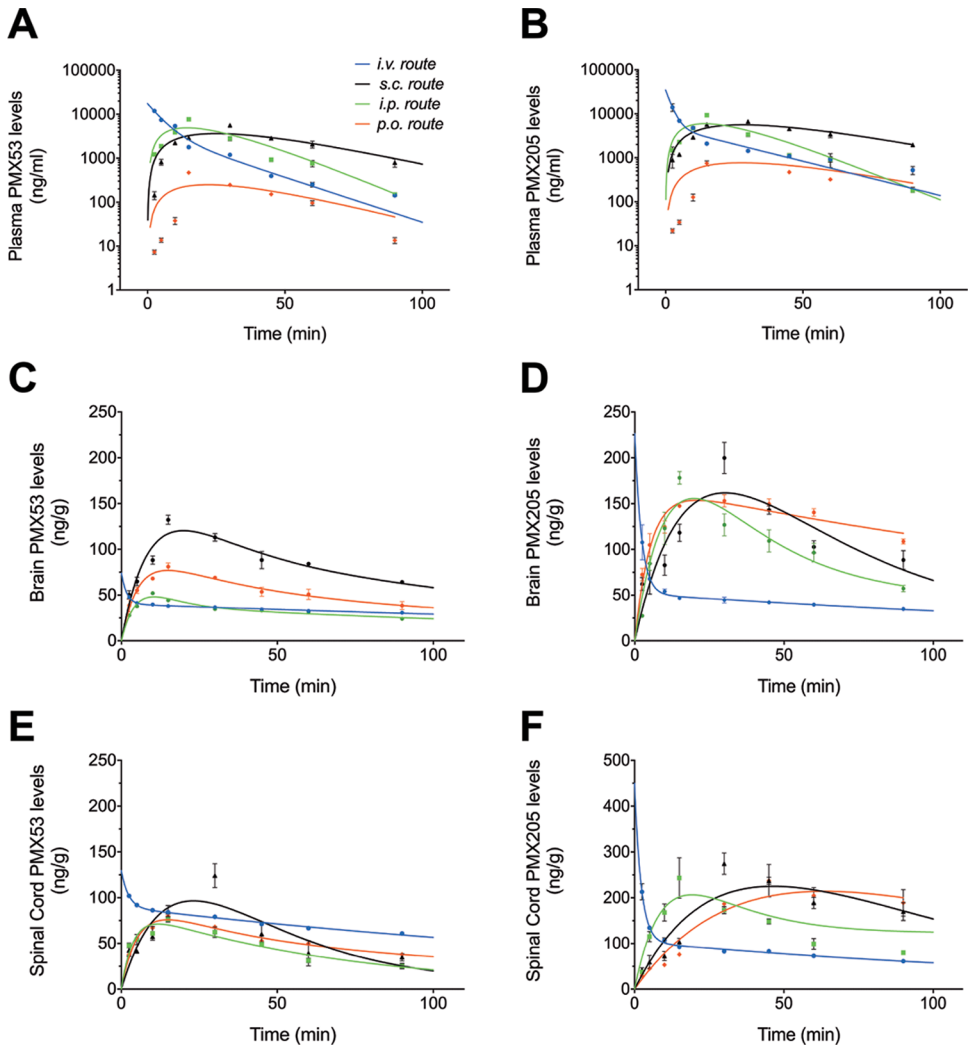

Figure 1. Concentration−time profile of complement C5a receptor 1 antagonists in wild-type mice following a single drug dose. Mice were administered a 1 mg/kg dose of PMX53 or PMX205 via intravenous (i.v.), intraperitoneal (i.p.), subcutaneous (s.c.), and per-oral (p.o.) routes. The concentration vs time profiles in plasma [(A), PMX53 and (B) PMX205], the brain [(C) PMX53 and (D) PMX205], and the spinal cord [(E) PMX53 and (F) PMX205] are shown. Dot points represent actual experimental values, and continuous lines represent predicted values generated by WINNONLIN (n = 4). Data are presented as mean ± SEM.

The concentration versus time profiles for PMX53 and PMX205 in plasma (Figure 1A,B), the brain (Figure 1C,D), and the spinal cord (Figure 1E,F) are shown following 1 mg/kg dosing via i.v., i.p., s.c., and p.o. routes of administration. Both PMX53 and PMX205 demonstrated a rapid distribution in the plasma, followed by elimination after i.v. dosing (Figure 1A,B). PMX205 had a shorter and faster distribution half-life and slightly improved elimination half-life (1.51 and 19.33 min) compared to PMX53 (3.49 and 14.73 min) following a single i.v. dose of 1 mg/kg, which may be due to the more lipophilic nature of PMX205. This trend was also observed in the brain (Figure 1C,D) and the spinal cord (Figure 1E,F). This is also reflected by shorter mean residence time (MRT) values for PMX205 (Tables 2 and 3). Additionally, brain and spinal cord elimination half-lives of PMX205 are shorter compared to those of PMX53, again, likely due to the more lipophilic nature of PMX205, supporting its increased permeability across blood−brain and blood−spinal cord barriers.

PMX53 peak plasma concentrations of 4.92, 3.77, and 0.25 μg/mL were observed at ∼14, ∼27, and ∼22 min via i.p., s.c., and p.o. routes of administration, respectively, at an administered dose of 1 mg/kg. Additionally, infinity predicted plasma mean residence times for PMX53 were ∼18, ∼36, ∼48, and ∼34 min following i.v., i.p., s.c., and p.o. routes, respectively. By contrast, calculated peak concentrations of PMX205 in plasma were ∼5.95, ∼5.62, and ∼0.77 μg/mL as observed at ∼14, ∼28, and ∼27 min via i.p., s.c., and p.o. routes of administration, respectively, at an administered dose of 1 mg/kg. For PMX205, the infinity predicted plasma mean residence times were ∼37, ∼26, ∼64, and ∼54 min following i.v., i.p., s.c., and p.o. routes, respectively. Peak brain and spinal cord levels of the C5aR1 antagonists correlated with time points of their corresponding plasma levels and were above their cellular IC_{50} concentration (PMX53: 26 nM and PMX205: 31 nM[10]). Overall, brain and spinal cord elimination half-lives of PMX53 were greater than those of PMX205 following i.v. drug administration, suggesting greater brain retention of PMX205.

Bioavailability results (Table 4) indicate that the plasma bioavailability of PMX53 is ∼9% via the p.o. route and ∼68% via the i.p. route. By comparison, PMX205 has better oral

https://dx.doi.org/10.1021/acsomega.9b03735
ACS Omega 2020, 5, 2345−2354

Table 4. Bioavailability and Drug Targeting Efficiency of Complement C5a Receptor 1 Antagonists

drug	route	area under curve (min μg/mL)	bioavailability	brain drug targeting efficiency	spinal cord drug targeting efficiency
PMX53	i.v.	150.63	100%		
	s.c.	134.45	85%	1.37	0.77
	i.p.	107.81	68.2%	0.71	0.63
	p.o.	13.64	8.6%	8.21	4.42
PMX205	i.v.	208.03	100%		
	s.c.	201.04	96.6%	1.71	1.37
	i.p.	125.50	60.3%	1.88	0.71
	p.o.	47.12	22.6%	10.81	8.21

bioavailability of >20% following p.o. dosing and an i.p. bioavailability of ∼60%. The s.c. bioavailability of PMX205 is greater compared to PMX53 (∼96% compared with ∼85%, respectively). Additionally, the drug targeting efficiency values of PMX53 and PMX205 as represented in Table 4 reflect the superior ability of PMX205 to target brain and spinal cord tissues to that of PMX53.

2.2. Repeat Dosing Pharmacokinetics of PMX205 in Wild-Type Mice. For the repeat dosing pharmacokinetics and accumulation studies, the lead clinical drug candidate, PMX205, was selected. Two specific routes were chosen based upon the pharmacokinetic profile of PMX205 (i.e. oral route and s.c. route). For the oral route, PMX205 was administrated through drinking water. This route of administration has been utilized by various groups to study the therapeutic benefit of PMX205 in neurodegenerative disease mouse models where chronic dosing is required.[4,15,16] Five-day pharmacokinetic results from mice that were administered PMX205 via the s.c. route (1 mg/kg) or via the drinking water (60 mg/L) are presented in Figure 2A,B, respectively. The results reveal that levels of PMX205 in plasma, the spinal cord, and the brain remain relatively unchanged over the 5 day treatment protocol, suggesting that no accumulation of compound occurs with this dosing regimen. After each 24 h interval, the levels of circulating PMX205 in plasma were very low, as expected from the predicted half-life of the acute dosing pharmacokinetic studies. Despite this low circulating level of PMX205, brain and spinal cord levels were comparatively higher. Importantly, the consistent and maintained levels of PMX205 in the CNS tissue are above the cell-based IC_{50} values for C5aR1 inhibition,[10,12] indicating daily s.c. administration, or drinking water administration of PMX205, is sufficient to block C5aR1 activation in the CNS.

Long-term pharmacokinetic studies were performed next to confirm PMX205 duration in brain tissue following a single i.v. dose of the compound over 120 h. Within the first 6 h of PMX205 administration, there was a significant reduction in brain levels due to clearance, and within 24 h, the majority of compounds that could produce any therapeutic effect were eliminated from the brain (Figure 2C). The data support the absence of any secondary uptake mechanisms that could lead to accumulation of PMX205 in the brain following administration.

2.3. Excretion Studies of PMX205. Elimination of PMX205 from mice was determined by calculating the amount of PMX205 excreted in an unchanged form through the urine or feces. Figure 3 illustrates that most of the PMX205 is excreted unchanged and primarily within the first 6 h following administration. Urinary excretion is the major route of elimination as indicated by high levels of unchanged PMX205 in urine samples collected over the 48 hour duration following i.v. administration (Figure 3A) and from the bladder just prior to euthanasia following p.o. administration (Figure 3B). Following i.v. administration, up to 46% of the PMX205 was excreted unchanged through urine and up to 16% via feces within the first 24 h (Figure 3C,D). Given this notable excretion of unchanged PMX205, we applied this to determine the effective oral bioavailability, in addition to the AUC ratio. Following equal amounts of compound administration, ∼4.2 ± 0.5 ng of detectable PMX205 was excreted out unchanged up to 90 min following p.o. dosing and ∼20.7 ± 3.8 ng of PMX205 over a period of 4 h after i.v. dosing. Accounting for these urinary excreted unchanged levels of PMX205, a calculated oral absorption of ∼20% was determined for PMX205.

Mice were administered PMX205 via intravenous (i.v.) or per-oral (p.o.) administration (1 mg/kg). Drug levels in the urine are shown for (A) 48 h for the i.v. route and (B) 90 min for the p.o. route. (C) Following i.v. administration, excretion of unchanged PMX205 (%) in urine was analyzed over 48 h with cumulative analysis presented at 4, 24, and 48 h. (D) Excretion of unchanged PMX205 (%) was also analyzed for the first 24 h in urine and feces following i.v. administration and compared with a dose control of 1 mg/kg per animal. Data points represent mean ± SEM of n = 5 mice at each time point.

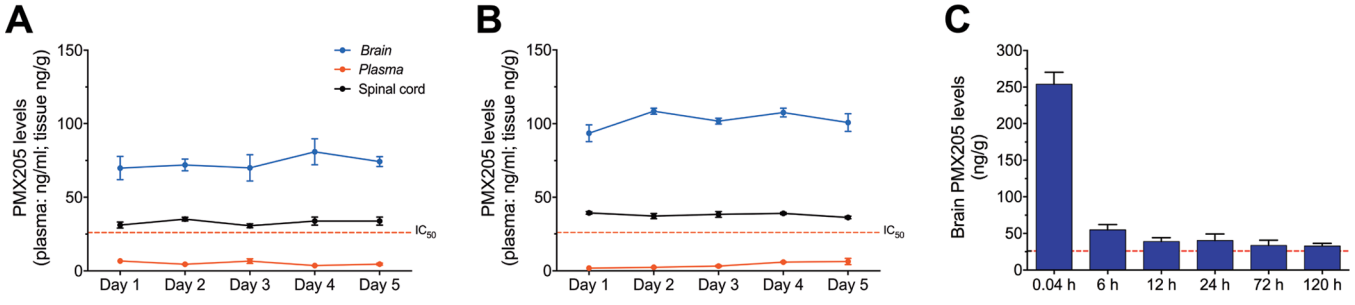

Figure 2. Repeated dosing pharmacokinetics of complement C5a receptor 1 (C5aR1) antagonist PMX205 in wild-type mice. Mice were administered PMX205 daily via subcutaneous (s.c.) administration (1 mg/kg) or via drinking water (60 mg/L) for 5 days. Drug levels in plasma, the brain, and the spinal cord at each 24 h time point following administration are shown for (A) the *s.c.* route and (B) drinking water route. (C) PMX205 levels in the brain up to 120 h following a single i.v. dose of 1 mg/kg PMX205. Data points represents mean ± SEM of n = 5 mice at each time point. Red dotted line represents cellular IC_{50} of the drug (31 nM; equivalent to ∼26 ng/mL) at the C5aR1.

https://dx.doi.org/10.1021/acsomega.9b03735
ACS Omega 2020, 5, 2345−2354

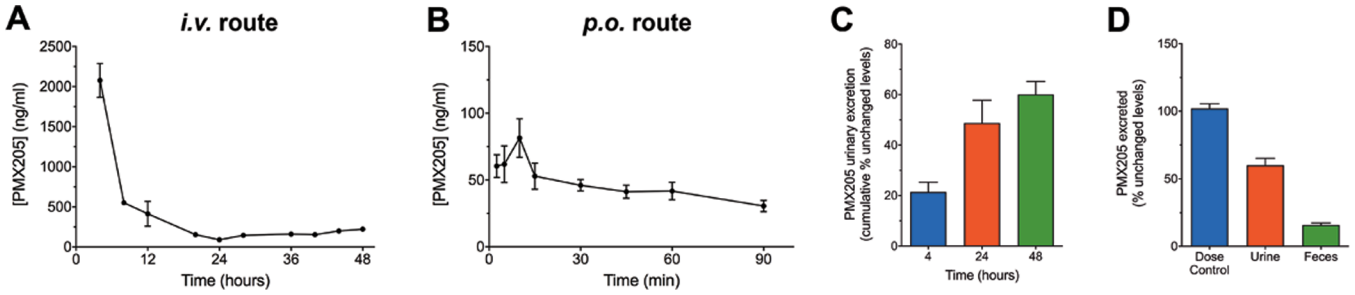

Figure 3. Excretion of complement C5a receptor 1 antagonist PMX205 in wild-type mice.

3. DISCUSSION

The cyclic peptide complement C5aR1 antagonists, PMX53 and PMX205, have been used extensively by various research groups in various species including mice, rats,[21] cats, dogs,[23] and humans.[24] Out of all the species, studies have been performed most extensively in mice, with >100 publications to date using these compounds for a number of diseases using a variety of administration routes in mice (e.g., i.v., s.c., i.p., p.o., drinking water, and others).[4−6,25−48] Despite this plethora of mouse studies using these compounds, only a few studies have performed pharmacokinetics, which are generally limited in scope and only examining one route of administration.[6,12,20−22] Furthermore, pharmacodynamics and therapeutic effects of drugs are difficult to correlate in the absence of pharmacokinetic data from various administration routes within the same species.

Results from the pharmacokinetic data performed in this study reveal the biphasic decline in plasma concentrations of PMX53 and PMX205 with rapid distribution and elimination profiles of both antagonists. Following i.v. administration of a single 1 mg/kg dose of either antagonist, the highest concentration in plasma, the brain, and tissue was observed after 2.5 min. Additionally, peak concentrations in CNS tissues corresponded to the peak levels in circulation as reflected by various routes for both antagonists. There was also rapid clearance of PMX205 from the circulation following i.v. dosing, with most compounds excreted in an unchanged form via urinary excretion. As expected, the plasma oral bioavailability of both PMX53 and PMX205 is lower than that in parenteral administration routes (∼10 and 20%, respectively), likely due to poor gastric and intestinal stability due to their peptidic nature.[13] Regardless, possibly due to the noncompetitive and pseudo-irreversible antagonist nature of the compound class,[12] oral dosing remains a viable mode of administration for this drug class in mice.[46]

In comparison to other routes of administration, the s.c. route resulted in improved bioavailability and maintained levels of antagonists in plasma, the brain, and the spinal cord for a longer duration, as reflected by plasma MRT values, absorption half-lives, and elimination half-lives. Drug targeting efficiency values, as calculated during pharmacokinetic studies, are helpful in the selection of drug candidates and routes of administration following comparative studies in the healthy state. Maximum potential therapeutic effects can be achieved in the disease state by administering drug candidates representing better drug targeting efficiency values via a selected route. Based on our data, the s.c. route represents the most viable route of administration for future clinical application of PMX205. In support of the clinical application of PMX205, repeat dosing (up to 5 days) and long-term dosing pharmacokinetic studies for this drug indicated no accumulation in the brain and spinal cord at the selected dose of 1 mg/kg and is well tolerated.

One area of future investigation will be to measure the "free" fraction of the drug in plasma and the CNS, to be able to accurately report the available concentrations of drug that could interact with unbound C5aR1. In addition to free fraction determination studies, future experiments are required to identify the rate, extent, and half-life equilibrium in the CNS to obtain a greater understanding of brain and spinal cord penetration and distribution of the antagonists. Finally, further studies are yet to be performed to correlate the drug availability with the length of duration in various non-CNS tissues.

4. CONCLUSIONS

In conclusion, a pharmacokinetic analysis of PMX53 and PMX205 was completed in mice following various routes of administration using a validated quantitative analysis method. The results demonstrate that both PMX53 and PMX205 express a rapid distribution and elimination profile, with renal excretion being the major route of elimination following i.v. administration. Repeat dosing and long-term experiments support the idea that PMX205 is well tolerated with no drug accumulation with repeat daily dosing. This pharmacokinetic data will be beneficial in correlating the drug therapeutic effects in mice with drug bioavailability and drug tissue availability. The current data indicate that the s.c. route of administration for PMX205 provides high bioavailability and prolonged plasma concentrations, coupled with high blood−brain barrier and blood-spinal cord barrier penetration, making this an ideal route for neurological diseases and clinical application.

5. MATERIALS AND METHODS

5.1. C5aR1 Antagonist Synthesis. C5aR1 cyclic peptidic antagonists were synthesized manually on 2-chlorotrityl resin (1.0 mmol g^{-1}, 0.25mmol scale) using Fmoc-based solid-phase chemistry. Couplings were performed using 2-(1*H*-benzotriazol-1-yl)-1,1,3,3-tetramethyluronium hexafluorophosphate with diisopropylethylamine (DIPEA) in *N*,*N*′-dimethylformamide (DMF). Peptides were N-terminally acetylated on resin by treatment with acetic anhydride (870 μL of acetic anhydride and 470 μL of DIPEA in 15 mL of DMF) followed by cleavage from the resin by treatment with a mixture of trifluoroacetic acid (TFA), triisopropylsilane, and water (95:2.5:2.5, 20 mL) for 1.5 h at 23 °C. The TFA was removed in vacuo, and the peptide was precipitated by addition of diethyl ether, collected by filtration, dissolved in buffer A/B (50:50) (A: water with 0.05% TFA; B: 90% acetonitrile, 10% water with 0.045% TFA), and lyophilized.

https://dx.doi.org/10.1021/acsomega.9b03735
ACS Omega 2020, 5, 2345−2354

The crude peptide was cyclized by dissolving the peptide in DMF (10 mM) with 5 equiv of (benzotriazol-1-yloxy)-tripyrrolidinophosphonium hexafluorophosphate, then 15 equiv of DIPEA was added, and the solution was stirred overnight at 23 °C. The DMF was then removed in vacuo, and the residue was redissolved in buffer A/B (50:50) and lyophilized. Peptides were purified by reverse-phase HPLC on a C_{18} column (Phenomenex Jupiter 300) using a gradient of 0−80% buffer B (in buffer A) over 80 min with UV monitoring at 214 and 280 nm. Electrospray mass spectroscopy confirmed the molecular mass of the peptide, and analytical reverse-phase HPLC was used to analyze purity.

5.2. Chemicals and Reagents. Acetonitrile (LC−MS grade), methanol (AR grade), and ethanol (AR grade) were sourced from Ajax FineChem (Australia). Formic acid (optima LC−MS grade) was purchased from Fisher Scientific (USA). Ultrapure deionized water was obtained from a Millipore Milli-Q water system (Millipore MA, USA). PMX53 and PMX205 solutions (10 mg/mL) were prepared by dissolving in sterile water for injection solution containing 5% ethanol and stored at −20 °C. On the day of experimentation, the required dose was prepared from drug stock in 5% dextrose in sterile water for injection and brought to 37 °C before administering to animals.

5.3. Animals. Animal care and all experimental procedures were performed following approval from the University of Queensland Animal Care and Use Committee and conducted in accordance with the National Health and Medical Research Council of Australia policies and guidelines for the care and use of animals for scientific purposes. Wild-type C57BL/6J mice (male, 10−12 weeks old) were purchased from Animal Resources Centre, Western Australia. All animals were housed within the University of Queensland Biological Resources animal facility in a pathogen-free environment with a 12 h dark/light cycle and free access ad libitum to food and water.

5.4. Pharmacokinetics of C5aR1 Antagonists. The pharmacokinetic profiles of C5aR1 antagonists were assessed via four routes of drug administration, that is, intravenous (i.v.; via tail vein), subcutaneous (s.c.; over shoulders), intraperitoneal (i.p.), and per-oral (p.o.; via oral gavage). Samples were collected and processed for PMX53 and PMX205 determination using a validated LC−MS/MS method as described previously.[13] Briefly, mice (n = 4) were anaesthetized with zolazepam (50 mg/kg) and xylazine (12 mg/kg) via i.p. injection. Anaesthetized mice were administered 1 mg/kg drug solution through the selected route. Blood samples were collected via a left ventricle cardiac puncture using a syringe loaded with 20 μL of 100 mM ethylenediaminetetraacetic acid (Sigma-Aldrich, St. Louis, MO) at 2.5, 5, 10, 15, 30, 45, 60, and 90 min, and plasma was extracted by centrifugation at 4000 rpm for 15 min at 4 °C. Following blood collection, mice were immediately perfused transcardially with normal saline to remove drug from the circulation in the brain and spinal cord. Whole brain and spinal cord samples were obtained and homogenized in equal weight volume of milliQ water. The tissue homogenate (100 μL) was mixed with 10 μL of 1 μg/mL internal standard (PMX53 for PMX205 studies and PMX205 for PMX53 studies), vortexed, and deproteinized with 1:3 ice cold LCMS-grade acetonitrile. Samples were sonicated followed by centrifugation at 13,000 × g for 30 min for supernatant collection and dried using a CentriVap sample concentrator at room temperature. Samples were stored at −80 °C for LC−MS/MS analysis. Plasma samples (50 μL) were also processed using the method described above. On the day of analysis, samples were suspended in 50 μL of 75% methanol/water and 10 μL was analyzed through a validated LC−MS/MS protocol.[13]

All the time points were terminal, and consequently, mean drug concentrations per time point were used for pharmacokinetics parameter determination using WINNONLIN software after suitable compartment model selection. A model selection was supported by the vascular (i.v. bolus) or extravascular (i.p., s.c., and p.o.) routes of drug administration. The linear trapezoidal rule was applied for calculation of the area under the curve (AUC) using the plasma concentration versus time profile of C5aR1 antagonists. Each antagonist's bioavailability was determined by comparing the ratio of AUC values of each drug via each specific route versus the AUC of the same antagonists via the i.v. route. In addition to this, zero−infinity predicted AUC values were also used to determine drug targeting efficiency. Higher drug targeting efficiency values reflect superior targeting of the drug to the specific tissue analysed[49] and are calculated as follows:

$$\text{drug targeting efficiency}_{(\text{i.p.})} = (\text{AUC}_{\text{tissue}}/\text{AUC}_{\text{plasma}})_{\text{i.p.}}/(\text{AUC}_{\text{tissue}}/\text{AUC}_{\text{plasma}})_{\text{i.v.}} \quad (1)$$

$$\text{drug targeting efficiency}_{(\text{p.o.})} = (\text{AUC}_{\text{tissue}}/\text{AUC}_{\text{plasma}})_{\text{p.o.}}/(\text{AUC}_{\text{tissue}}/\text{AUC}_{\text{plasma}})_{\text{i.v}} \quad (2)$$

$$\text{drug targeting efficiency}_{(\text{s.c.})} = (\text{AUC}_{\text{tissue}}/\text{AUC}_{\text{plasma}})_{\text{s.c.}}/(\text{AUC}_{\text{tissue}}/\text{AUC}_{\text{plasma}})_{\text{i.v}} \quad (3)$$

5.5. Repeat Dosing Pharmacokinetics of C5aR1 Antagonist. For the drinking water group, C57BL/6J mice (n = 5) were kept in a controlled 12 h light/dark cycle environment for up to 5 days with free access to food and water containing 60 mg/L of PMX205. On days 1, 2, 3, 4, and 5, plasma and tissue samples were collected 2 h after the start of the dark cycle. The amount of water intake was monitored each day, and the total water consumption was recorded at the end of the fifth experimental day. For the s.c. route group, C57BL/6J mice (n = 5) were administered PMX205 1 mg/kg s.c. daily at an interval of 24 h. Plasma and tissue samples were collected for analysis on days 1, 2, 3, 4, and 5. Samples were processed and analyzed for PMX205 levels using the LC−MS/MS. For the single i.v. route, C57BL/6J mice (n = 4) were dosed 1 mg/kg PMX205 i.v. and kept in metabolic cages (Tecniplast; 3600M021) for up to 120 h. Brain samples were collected at 0.04 (2.5 min), 6, 12, 2, 72, and 120 h. Samples were processed and analyzed for PMX205 levels as described above.

5.6. Excretion Studies of C5aR1 Antagonist. Excretion studies were performed in metabolic cages using C57BL/6J mice (n = 5). Mice were administered PMX205 (1 mg/kg) i.v. and kept in metabolic cages for the duration of 48 h. Urine and feces samples were collected at 4 h intervals and stored at −80 °C. For excretion studies following the p.o. route, mice were administered 1 mg/kg PMX205 via oral gavage and samples were collected at different time intervals from the urinary bladder prior to perfusion. On the day of analysis, samples

https://dx.doi.org/10.1021/acsomega.9b03735
ACS Omega 2020, 5, 2345−2354

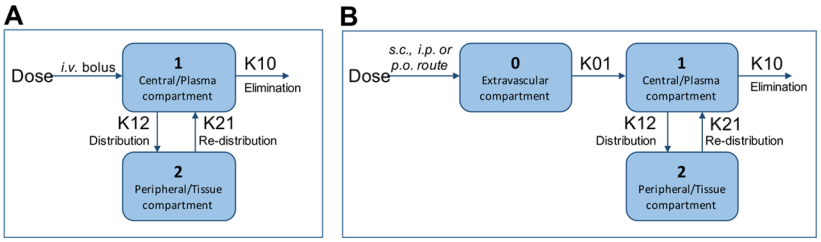

Figure 4. Two-compartment pharmacokinetic models used in this study. (A) Pharmacokinetics model for the intravenous (i.v.) route with a bolus drug administration at time $t = 0$. (B) Pharmacokinetic model for the extravascular route, with no lag time, first order input, and first order output used for intraperitoneal (i.p.), subcutaneous (s.c.), and per-oral (p.o.) routes of drug administration.

were process and analyzed using the validated LC−MS/MS method.

5.7. Data Analysis. All results are reported as mean ± standard error of mean using GraphPad Prism (software version 7.0, LaJolla, CA). Pharmacokinetics data analysis was performed using Pharsight Phoenix WINNONLIN software (version 6.4), the industry standard for pharmacokinetic/pharmacodynamic modeling, analysis, and simulation. A two-compartmental analysis method was used to obtain various pharmacokinetic parameters. Figure 4A,B represents the model used for intravenous drug administration and for all extravascular routes of drug administration following a single dose of antagonists at 1 mg/kg. Fitness of the pharmacokinetic model was assessed using the WINONLIN criterion and by a graph plot of observed and predicted concentrations versus time. Results are also expressed by graph plots of predicted concentration values versus observed concentration values and changes of partial derivatives with time with or without clearance parameters.

AUTHOR INFORMATION

Corresponding Author

Trent M. Woodruff − *School of Biomedical Sciences, The University of Queensland, St Lucia, Brisbane 4072, Australia; Wesley Medical Research, The Wesley Hospital, Auchenflower, Brisbane 4066, Australia;* orcid.org/0000-0003-1382-911X; Phone: +61-7-336 52924; Email: t.woodruff@uq.edu.au; Fax: +61-7-336-51766

Authors

Vinod Kumar − *School of Biomedical Sciences, The University of Queensland, St Lucia, Brisbane 4072, Australia*

John D. Lee − *School of Biomedical Sciences, The University of Queensland, St Lucia, Brisbane 4072, Australia; University of Queensland Centre for Clinical Research, the University of Queensland, Brisbane 4029, Australia*

Richard J. Clark − *School of Biomedical Sciences, The University of Queensland, St Lucia, Brisbane 4072, Australia;* orcid.org/0000-0002-6807-5426

Peter G. Noakes − *School of Biomedical Sciences, The University of Queensland, St Lucia, Brisbane 4072, Australia; Queensland Brain Institute, the University of Queensland, St Lucia, Brisbane 4072, Australia*

Stephen M. Taylor − *School of Biomedical Sciences, The University of Queensland, St Lucia, Brisbane 4072, Australia*

Complete contact information is available at: https://pubs.acs.org/10.1021/acsomega.9b03735

Author Contributions

V.K., J.D.L., R.J.C., P.G.N., S.M.T., and T.M.W. participated in research design. V.K. conducted the experiments. V.K., J.D.L., R.J.C., and T.M.W. analyzed the data. V.K., J.D.L., and T.M.W. wrote or contributed to the writing of the manuscript. All authors read and approved the final manuscript.

Notes

The authors declare the following competing financial interest(s): Prof Woodruff consults to Alsonex Pty Ltd, who are commercially developing PMX205 for ALS treatment. He holds no stocks, shares or other commercial interest in this company.

ACKNOWLEDGMENTS

The authors would like to thank Dr. Alan Robertson for his insightful comments to improve the manuscript. The research was supported by funding from an Advance Queensland Innovation Partnership grant and a National Health and Medical Research Council (NHMRC) Development grant (APP1118881). T.M.W. is supported by an NHMRC Career Development Fellowship (APP1105420) and J.D.L. by a Motor Neuron Disease Research Institute of Australia Postdoctoral Fellowship (PDF1604).

ABBREVIATIONS

AUC, area under the curve; C5aR1, C5a receptor 1; C5aR2, C5a receptor-like 2; CNS, central nervous system; DIPEA, diisopropylethylamine; DMF, *N*,*N*′-dimethylformamide; i.p., intraperitoneal; i.v., intravenous; MRT, mean residence time; p.o., per-oral; s.c., subcutaneous; TFA, trifluoroacetic acid

REFERENCES

(1) Kjældgaard, A.-L.; Pilely, K.; Olsen, K. S.; Pedersen, S. W.; Lauritsen, A. Ø.; Møller, K.; Garred, P. Amyotrophic lateral sclerosis: The complement and inflammatory hypothesis. *Mol. Immunol.* **2018**, *102*, 14−25.

(2) Brennan, F. H.; Lee, J. D.; Ruitenberg, M. J.; Woodruff, T. M. Therapeutic targeting of complement to modify disease course and improve outcomes in neurological conditions. *Semin. Immunol.* **2016**, *28*, 292−308.

(3) Li, R.; Coulthard, L. G.; Wu, M. C. L.; Taylor, S. M.; Woodruff, T. M. C5L2: a controversial receptor of complement anaphylatoxin, C5a. *FASEB J* **2013**, *27*, 855−864.

(4) Lee, J. D.; Kumar, V.; Fung, J. N. T.; Ruitenberg, M. J.; Noakes, P. G.; Woodruff, T. M. Pharmacological inhibition of complement C5a-C5a$_1$ receptor signalling ameliorates disease pathology in the hSOD1^{G93A} mouse model of amyotrophic lateral sclerosis. *Br. J. Pharmacol.* **2017**, *174*, 689−699.

(5) Brennan, F. H.; Gordon, R.; Lao, H. W.; Biggins, P. J.; Taylor, S. M.; Franklin, R. J. M.; Woodruff, T. M.; Ruitenberg, M. J. The complement receptor C5aR controls acute inflammation and

astrogliosis following spinal cord injury. *J. Neurosci.* **2015**, *35*, 6517−6531.
(6) Benson, M. J.; Thomas, N. K.; Talwar, S.; Hodson, M. P.; Lynch, J. W.; Woodruff, T. M.; Borges, K. A novel anticonvulsant mechanism via inhibition of complement receptor C5ar1 in murine epilepsy models. *Neurobiol. Dis.* **2015**, *76*, 87−97.
(7) Woodruff, T. M.; Crane, J. W.; Proctor, L. M.; Buller, K. M.; Shek, A. B.; de Vos, K.; Pollitt, S.; Williams, H. M.; Shiels, I. A.; Monk, P. N.; Taylor, S. M. Therapeutic activity of C5a receptor antagonists in a rat model of neurodegeneration. *FASEB J* **2006**, *20*, 1407−1417.
(8) Hawksworth, O. A.; Li, X. X.; Coulthard, L. G.; Wolvetang, E. J.; Woodruff, T. M. New concepts on the therapeutic control of complement anaphylatoxin receptors. *Mol. Immunol.* **2017**, *89*, 36−43.
(9) Finch, A. M.; Wong, A. K.; Paczkowski, N. J.; Wadi, S. K.; Craik, D. J.; Fairlie, D. P.; Taylor, S. M. Low-molecular-weight peptidic and cyclic antagonists of the receptor for the complement factor C5a. *J. Med. Chem.* **1999**, *42*, 1965−1974.
(10) March, D. R.; Proctor, L. M.; Stoermer, M. J.; Sbaglia, R.; Abbenante, G.; Reid, R. C.; Woodruff, T. M.; Wadi, K.; Paczkowski, N.; Tyndall, J. D. A.; Taylor, S. M.; Fairlie, D. P. Potent cyclic antagonists of the complement C5a receptor on human polymorphonuclear leukocytes. Relationships between structures and activity. *Mol. Pharmacol.* **2004**, *65*, 868−879.
(11) Woodruff, T. M.; Costantini, K. J.; Crane, J. W.; Atkin, J. D.; Monk, P. N.; Taylor, S. M.; Noakes, P. G. The complement factor C5a contributes to pathology in a rat model of amyotrophic lateral sclerosis. *J. Immunol.* **2008**, *181*, 8727−8734.
(12) Woodruff, T. M.; Pollitt, S.; Proctor, L. M.; Stocks, S. Z.; Manthey, H. D.; Williams, H. M.; Mahadevan, I. B.; Shiels, I. A.; Taylor, S. M. Increased potency of a novel complement factor 5a receptor antagonist in a rat model of inflammatory bowel disease. *J. Pharmacol. Exp. Ther.* **2005**, *314*, 811−817.
(13) Kumar, V.; Lee, J. D.; Clark, R. J.; Woodruff, T. M. Development and validation of a LC-MS/MS assay for pharmacokinetic studies of complement C5a receptor antagonists PMX53 and PMX205 in mice. *Sci. Rep.* **2018**, *8*, 8101.
(14) Biggins, P. J. C.; Brennan, F. H.; Taylor, S. M.; Woodruff, T. M.; Ruitenberg, M. J. The Alternative Receptor for Complement Component 5a, C5aR2, Conveys Neuroprotection in Traumatic Spinal Cord Injury. *J. Neurotrauma* **2017**, *34*, 2075−2085.
(15) Ager, R. R.; Fonseca, M. I.; Chu, S.-H.; Sanderson, S. D.; Taylor, S. M.; Woodruff, T. M.; Tenner, A. J. Microglial C5aR (CD88) expression correlates with amyloid-β deposition in murine models of Alzheimer's disease. *J. Neurochem.* **2010**, *113*, 389−401.
(16) Fonseca, M. I.; Ager, R. R.; Chu, S.-H.; Yazan, O.; Sanderson, S. D.; LaFerla, F. M.; Taylor, S. M.; Woodruff, T. M.; Tenner, A. J. Treatment with a C5aR antagonist decreases pathology and enhances behavioral performance in murine models of Alzheimer's disease. *J. Immunol.* **2009**, *183*, 1375−1383.
(17) Strachan, A. J.; Shiels, I. A.; Reid, R. C.; Fairlie, D. P.; Taylor, S. M. Inhibition of immune-complex mediated dermal inflammation in rats following either oral or topical administration of a small molecule C5a receptor antagonist. *Br. J. Pharmacol.* **2001**, *134*, 1778−1786.
(18) Paczkowski, N. J.; Finch, A. M.; Whitmore, J. B.; Short, A. J.; Wong, A. K.; Monk, P. N.; Cain, S. A.; Fairlie, D. P.; Taylor, S. M. Pharmacological characterization of antagonists of the C5a receptor. *Br. J. Pharmacol.* **1999**, *128*, 1461−1466.
(19) Köhl, J. Drug evaluation: the C5a receptor antagonist PMX-53. *Curr. Opin. Mol. Ther.* **2006**, *8*, 529−538.
(20) Seow, V.; Lim, J.; Cotterell, A. J.; Yau, M.-K.; Xu, W.; Lohman, R.-J.; Kok, W. M.; Stoermer, M. J.; Sweet, M. J.; Reid, R. C.; Suen, J. Y.; Fairlie, D. P. Receptor residence time trumps drug-likeness and oral bioavailability in determining efficacy of complement C5a antagonists. *Sci. Rep.* **2016**, *6*, 24575.
(21) Morgan, M.; Bulmer, A. C.; Woodruff, T. M.; Proctor, L. M.; Williams, H. M.; Stocks, S. Z.; Pollitt, S.; Taylor, S. M.; Shiels, I. A. Pharmacokinetics of a C5a receptor antagonist in the rat after different sites of enteral administration. *Eur. J. Pharm. Sci.* **2008**, *33*, 390−398.
(22) Strachan, A. J.; Woodruff, T. M.; Haaima, G.; Fairlie, D. P.; Taylor, S. M. A new small molecule C5a receptor antagonist inhibits the reverse-passive Arthus reaction and endotoxic shock in rats. *J. Immunol.* **2000**, *164*, 6560−6565.
(23) Shiels, I. A. A complement C5a antagonist for antiinflammatory therapy in veterinary practice. In *Australian College of Veterinary Scientist-Science week 2005-Small animal medicine chapter meeting*; 2005.
(24) Vergunst, C. E.; Gerlag, D. M.; Dinant, H.; Schulz, L.; Vinkenoog, M.; Smeets, T. J. M.; Sanders, M. E.; Reedquist, K. A.; Tak, P. P. Blocking the receptor for C5a in patients with rheumatoid arthritis does not reduce synovial inflammation. *Rheumatology (Oxford, U. K.)* **2007**, *46*, 1773−1778.
(25) Karsten, C. M.; Beckmann, T.; Holtsche, M. M.; Tillmann, J.; Tofern, S.; Schulze, F. S.; Heppe, E. N.; Ludwig, R. J.; Zillikens, D.; König, I. R.; Köhl, J.; Schmidt, E. Tissue Destruction in Bullous Pemphigoid Can Be Complement Independent and May Be Mitigated by C5aR2. *Front. Immunol.* **2018**, *9*, 488.
(26) Dick, J.; Gan, P.-Y.; Ford, S. L.; Odobasic, D.; Alikhan, M. A.; Loosen, S. H.; Hall, P.; Westhorpe, C. L.; Li, A.; Ooi, J. D.; Woodruff, T. M.; Mackay, C. R.; Kitching, A. R.; Hickey, M. J.; Holdsworth, S. R. C5a receptor 1 promotes autoimmunity, neutrophil dysfunction and injury in experimental anti-myeloperoxidase glomerulonephritis. *Kidney Int.* **2018**, *93*, 615−625.
(27) Zha, H.; Han, X.; Zhu, Y.; Yang, F.; Li, Y.; Li, Q.; Guo, B.; Zhu, B. Blocking C5aR signaling promotes the anti-tumor efficacy of PD-1/PD-L1 blockade. *Oncoimmunology* **2017**, *6*, No. e1349587.
(28) Khor, K. H.; Moore, T. A.; Shiels, I. A.; Greer, R. M.; Arumugam, T. V.; Mills, P. C. A Potential Link between the C5a Receptor 1 and the β1-Adrenoreceptor in the Mouse Heart. *PLoS One* **2016**, *11*, No. e0146022.
(29) Zhang, C.; Li, Y.; Wang, C.; Wu, Y.; Du, J. Antagonist of C5aR prevents cardiac remodeling in angiotensin II-induced hypertension. *Am. J. Hypertens.* **2014**, *27*, 857−864.
(30) Denny, K. J.; Coulthard, L. G.; Jeanes, A.; Lisgo, S.; Simmons, D. G.; Callaway, L. K.; Wlodarczyk, B.; Finnell, R. H.; Woodruff, T. M.; Taylor, S. M. C5a receptor signaling prevents folate deficiency-induced neural tube defects in mice. *J. Immunol.* **2013**, *190*, 3493−3499.
(31) Wu, M. C. L.; Brennan, F. H.; Lynch, J. P. L.; Mantovani, S.; Phipps, S.; Wetsel, R. A.; Ruitenberg, M. J.; Taylor, S. M.; Woodruff, T. M. The receptor for complement component C3a mediates protection from intestinal ischemia-reperfusion injuries by inhibiting neutrophil mobilization. *Proc. Natl. Acad. Sci. U. S. A.* **2013**, *110*, 9439−9444.
(32) Abe, T.; Hosur, K. B.; Hajishengallis, E.; Reis, E. S.; Ricklin, D.; Lambris, J. D.; Hajishengallis, G. Local complement-targeted intervention in periodontitis: proof-of-concept using a C5a receptor (CD88) antagonist. *J. Immunol.* **2012**, *189*, 5442−5448.
(33) Jang, J. H.; Liang, D.; Kido, K.; Sun, Y.; Clark, D. J.; Brennan, T. J. Increased local concentration of complement C5a contributes to incisional pain in mice. *J Neuroinflammation* **2011**, *8*, 80.
(34) Suetsugu-Maki, R.; Maki, N.; Fox, T. P.; Nakamura, K.; Cowper Solari, R.; Tomlinson, C. R.; Qu, H.; Lambris, J. D.; Tsonis, P. A. A complement receptor C5a antagonist regulates epithelial to mesenchymal transition and crystallin expression after lens cataract surgery in mice. *Mol Vis* **2011**, *17*, 949−964.
(35) Manthey, H. D.; Thomas, A. C.; Shiels, I. A.; Zernecke, A.; Woodruff, T. M.; Rolfe, B.; Taylor, S. M. Complement C5a inhibition reduces atherosclerosis in ApoE−/− mice. *FASEB J* **2011**, *25*, 2447−2455.
(36) Kim, G. H.; Mocco, J.; Hahn, D. K.; Kellner, C. P.; Komotar, R. J.; Ducruet, A. F.; Mack, W. J.; Connolly, E. S., Jr. Protective effect of C5a receptor inhibition after murine reperfused stroke. *Neurosurg.* **2008**, *63*, 122−126.
(37) Clark, J. D.; Qiao, Y.; Li, X.; Shi, X.; Angst, M. S.; Yeomans, D. C. Blockade of the complement C5a receptor reduces incisional

https://dx.doi.org/10.1021/acsomega.9b03735
ACS Omega 2020, 5, 2345−2354

allodynia, edema, and cytokine expression. *Anesthesiology* **2006**, *104*, 1274−1282.
(38) Kim, A. H. J.; Dimitriou, I. D.; Holland, M. C. H.; Mastellos, D.; Mueller, Y. M.; Altman, J. D.; Lambris, J. D.; Katsikis, P. D. Complement C5a receptor is essential for the optimal generation of antiviral CD8+ T cell responses. *J. Immunol.* **2004**, *173*, 2524−2529.
(39) Hillebrandt, S.; Wasmuth, H. E.; Weiskirchen, R.; Hellerbrand, C.; Keppeler, H.; Werth, A.; Schirin-Sokhan, R.; Wilkens, G.; Geier, A.; Lorenzen, J.; Köhl, J.; Gressner, A. M.; Matern, S.; Lammert, F. Complement factor 5 is a quantitative trait gene that modifies liver fibrogenesis in mice and humans. *Nat. Genet.* **2005**, *37*, 835−843.
(40) Fleming, S. D.; Mastellos, D.; Karpel-Massler, G.; Shea-Donohue, T.; Lambris, J. D.; Tsokos, G. C. C5a causes limited, polymorphonuclear cell-independent, mesenteric ischemia/reperfusion-induced injury. *Clin. Immunol.* **2003**, *108*, 263−273.
(41) Girardi, G.; Berman, J.; Redecha, P.; Spruce, L.; Thurman, J. M.; Kraus, D.; Hollmann, T. J.; Casali, P.; Caroll, M. C.; Wetsel, R. A.; Lambris, J. D.; Holers, V. M.; Salmon, J. E. Complement C5a receptors and neutrophils mediate fetal injury in the antiphospholipid syndrome. *J. Clin. Invest.* **2003**, *112*, 1644−1654.
(42) Huber-Lang, M. S.; Riedeman, N. C.; Sarma, J. V.; Younkin, E. M.; McGuire, S. R.; Laudes, I. J.; Lu, K. T.; Guo, R.-F.; Neff, T. A.; Padgaonkar, V. A.; Lambris, J. D.; Spruce, L.; Mastellos, D.; Zetoune, F. S.; Ward, P. A. Protection of innate immunity by C5aR antagonist in septic mice. *FASEB J* **2002**, *16*, 1567−1574.
(43) Herrmann, J. B.; Muenstermann, M.; Strobel, L.; Schubert-Unkmeir, A.; Woodruff, T. M.; Gray-Owen, S. D.; Klos, A.; Johswich, K. O. Complement C5a Receptor 1 Exacerbates the Pathophysiology of N. meningitidis Sepsis and Is a Potential Target for Disease Treatment. *MBio* **2018**, *9*, No. e01755-17.
(44) Mizuno, T.; Yoshioka, K.; Mizuno, M.; Shimizu, M.; Nagano, F.; Okuda, T.; Tsuboi, N.; Maruyama, S.; Nagamatsu, T.; Imai, M. Complement component 5 promotes lethal thrombosis. *Sci. Rep.* **2017**, *7*, 42714.
(45) Staab, E. B.; Sanderson, S. D.; Wells, S. M.; Poole, J. A. Treatment with the C5a receptor/CD88 antagonist PMX205 reduces inflammation in a murine model of allergic asthma. *Int. Immunopharmacol.* **2014**, *21*, 293−300.
(46) Jain, U.; Woodruff, T. M.; Stadnyk, A. W. The C5a receptor antagonist PMX205 ameliorates experimentally induced colitis associated with increased IL-4 and IL-10. *Br. J. Pharmacol.* **2013**, *168*, 488−501.
(47) de Vries, M. R.; Wezel, A.; Schepers, A.; van Santbrink, P. J.; Woodruff, T. M.; Niessen, H. W. M.; Hamming, J. F.; Kuiper, J.; Bot, I.; Quax, P. H. A. Complement factor C5a as mast cell activator mediates vascular remodelling in vein graft disease. *Cardiovasc. Res.* **2013**, *97*, 311−320.
(48) Verghese, D. A.; Chun, N.; Paz, K.; Fribourg, M.; Woodruff, T. M.; Flynn, R.; Hu, Y.; Xiong, H.; Zhang, W.; Yi, Z.; Du, J.; Blazar, B. R.; Heeger, P. S. C5aR1 regulates T follicular helper differentiation and chronic graft-versus-host disease bronchiolitis obliterans. *JCI Insight* **2018**, *3*, 124646.
(49) Meng, D.; Lu, H.; Huang, S.; Wei, M.; Ding, P.; Xiao, X.; Xu, Y.; Wu, C. Comparative pharmacokinetics of tetramethylpyrazine phosphate in rat plasma and extracellular fluid of brain after intranasal, intragastric and intravenous administration. *Acta Pharm. Sin. B* **2014**, *4*, 74−78.

https://dx.doi.org/10.1021/acsomega.9b03735
ACS Omega 2020, 5, 2345−2354